CHAPTER 1

INTRODUCTION

This chapter firstly outlines the principle and rationale of this work. Basic properties of tin dioxide and molybdenum trioxide, which are the materials selected for this work, will then be introduced and finally the objectives and usefulness.

1.1 Principles and rationales

Electronic nose (e–nose) systems have attracted much attention due to their potential applications in such area as food quality control, medical diagnosis, and environmental pollutant monitoring [1–4]. E–nose systems are useful for analyzing, classifying, or identifying complex chemical mixtures such as perfume, food, beverage, illness diagnosis etc., as shown in Fig. 1.1. The main purpose of the current research was to develop an instrument that could mimic the human sense of smell and provide rapid sensory information.

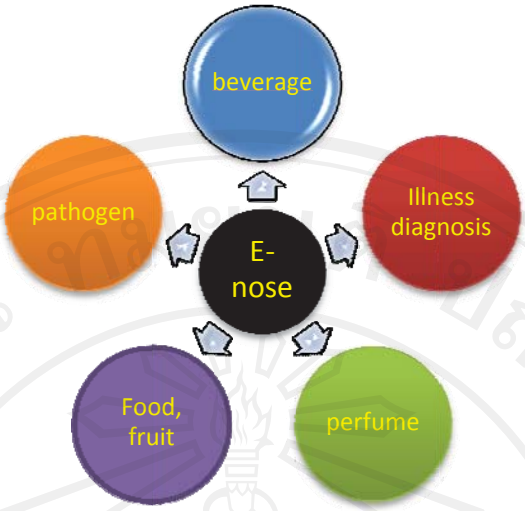

Figure 1.1 Applications of the electronic nose

The term ‘‘E–nose’’ is most commonly used in the literature to refer to this type of instrument, although other terms are also used, such as artificial nose, mechanical nose, odor–sensing system or electronic olfactometry. In the 1980s, Gardner and Bartlett [5] defined the e–nose as ‘‘an instrument, which comprises an array of electronic chemical sensors with partial specificity and an appropriate pattern–recognition system, capable of recognizing simple or complex odors’’. Although the definition was appropriate at that time, nowadays it does not include all the e–nose systems that are available on the market. At the end of the 1990s, a new type of the e–nose based on mass spectrometry (MS) was developed [6]. Even though some researchers do not consider that the MS–based system is an e–nose [7], the purpose of this new instrument, like the classical ones, is to differentiate and subsequently to classify samples according to their volatile composition in a fast and simple way. Therefore, the e–nose systems developed so far can be classified into two

groups on the basis of their detection systems [8]: classical instruments, which are based on solid state gas sensors, and new instruments, which are based on mass spectrometry (MS). The concept of the e–nose or the intelligent arrayed gas sensor system was first realized more than 20 years ago by Persaud and Dodd [9]. The earliest publication about instruments for odor assessment appeared at the beginning of the 1980s [10].

In the instruments developed, the volatile compounds interact with an array of gas sensors. Each gas sensor responds more selectively to a certain group of chemical compounds but also shows a broad, overlapping response to the others (cross–selectivity). In this way, a small number of the gas sensors (usually 8–32) can respond to a variety of different complex odors and there is no need to have one specific sensor for each individual compound. In a subsequent step, the data are processed with chemometric techniques such as principal component analysis (PCA), linear discriminant analysis (LDA), artificial neuron network (ANN) etc., in order to compare and/or to classify the samples according to their volatile compositions. This technique does not provide information on the amounts of the individual aroma compounds; rather, it makes a global, qualitative estimation of the aroma profile. In this respect, it is similar to human olfactory perception.

The general principle of the e–nose technique [8] is that the volatile compounds in the headspace of the sample are introduced into a detection system. Then, for each sample analyzed, the detector generates a set of signals that contains information about the volatile compositions of the sample. This set of signals is like a ‘‘fingerprint’’ of the sample analyzed. When several samples are analyzed, a data

matrix is generated that is subsequently treated with chemometric techniques so that the samples can be compared on the basis of their volatile compositions, and classified or discriminated depending on their origin, variety, purity, ripeness, aging, or any other properties of interest. When these statistical techniques are used, it should be borne in mind that results will be reliable only if a significant number of the samples of interest from the different categories of the property are analyzed. However, this is not a drawback, because the e–noses are simple to use and provide fast responses.

At present, there are continuous efforts to improve the e–nose systems even though several desk–top or hand–held products are commercially available, as shown in Fig. 1.2. In particular, a miniaturized and intelligent e–nose module could become a promising microfabricated component and possibly integrate into the personal mobile phone as digital cameras have been done. To fulfill this purpose, the small e–nose must satisfy additional requirements such as low–power consumption and mass productivity through batch fabrication, together with sufficient sensing abilities in terms of sensitivity and selectivity. Moreover, speed and simplicity are two important characteristics of the e–noses.

(a) (b)

Figure 1.2 Commercial electronic nose (a) desk–top and (b) mobile [11].

Metal oxide sensors have been utilized for several decades for low–cost detection of combustible and toxic gases. Many efforts have been focused on the development of the sensors to identify certain specific gases such as CO_2, CO, C_2H_5OH, CH_4, H_2, H_2S, etc. Most of those developments were based on semiconductor materials because of their small size, simple operation, high sensitivity and selectivity.

It has been known that the electrical properties of many semiconductors are sensitive to the gaseous ambient (H_2, CH_4, CO, CO_2, O_2, etc.). Metal oxides used as sensing materials in the semiconductor gas sensors have a wide band gap, typical for insulators. They possess conductivity in the range of semiconductors due to point defects in the crystal structure. The fundamental sensing mechanism of the metal oxide based gas sensors relies on a change in electrical conductivity due to the

interaction process between surface complexes such as O^-, O^{2-}, H^+, and OH^- reactive chemical species and the gas molecules to be detected. Since SnO_2 was first demonstrated as a gas sensing device in 1962 [12], much effort has been made to elucidate its ability to detect various toxic and flammable gases. Several studies [13] have focused on the capacity of dopants in the SnO_2 layer to increase the sensitivity of the sensor in detecting gases. According in these reports, the SnO_2 sensors operate only at high temperatures, such as 200–500°C. In particular, development of the sensors is to control sensing mechanisms into the three "S", sensitivity, selectivity and stability, of sensor technology.

One–dimensional (1D) metal oxide nanostructures, Si nanowires [14] and ZnO nanobelts [15], have attracted much attention due to their great potential applications, such as materials for solid–state gas sensors with great potential for overcoming the fundamental limitations due to their ultrahigh surface–to–volume ratio. Recently, gas sensors based on an individual carbon nanotube, SnO_2 and In_2O_3 nanowire have been fabricated [16–18]. These sensors have excellent response and recover characteristics. SnO_2 nanobelts were used as the gas sensing material, overcoming the difficulty of processing an individual nanowire/nanobelt [19]. Nanowire–based sensors and arrays of metal, metal oxide and conducting polymer have been fabricated using electrodeposition technique for biomolecular sensor [20]. Li et al. reported molecular detection based on electrodeposited copper nanowires grown between nano–gap electrodes [21]. Star et al. demonstrated carbon nanotube based FET devices [22].

E–noses have been used to evaluate the quality of modified atmosphere packaged poultry meat, spoiled beef, fish, milk and olive oil [23]. As far as the beverage field is concerned, the e–nose was used to discriminate four types of red wines which were made from the same variety of grapes and came from the same cellar. Successful discrimination of different Spanish wines made from different grapes using the e–nose was reported so far. The e–noses have also been widely used for the quality monitor of all kinds of fruits, such as mandarins, oranges, melons, blueberries, pears, and peaches [24, 25]. Experimental datasets were obtained and analyzed almost by the methods of PCA, LDA and ANN. However, only limited detailed information is available on the influence of experimental factors (the volume of vial and the headspace generated time) on the discrimination. A number of other different applications using the e–noses have been reported, e.g. quality estimation of ground meat, monitoring beer production, analysis of accelerants and fire debris, and discrimination of different types of teas [26, 27].

A number of gas sensors with different sensing characteristic are required to improve the performance of the e–nose. Chemometric or statistical technique is still the case study for improvement of the e–nose's ability. To understand how the e–nose works, this work aims to fabricate an array–based gas sensor. Wide band gap semiconductors SnO_2 and MoO_3, are to be used for this study. Therefore, the basic properties of these materials will be introduced.

1.2 Basic properties of MoO_3 and SnO_2

1.2.1 Molybdenum trioxide

Molybdenum trioxide (MoO_3) occurs in the rare mineral molybdite. It is used to manufacture molybdenum metal and as catalyst to synthesize the industrially valuable products like acrylonitrile and acrylic acid [28-29]. It dissolves slightly in water to give molybdic acid. MoO_3 occurs in slightly blue color for the powder form and its single crystal is transparent. The energy gap of MoO_3 is about 3.0 eV and its sublimation temperature begins at about 700°C. Its melting and boiling point are 795°C and 1150°C, respectively. Physical properties of α–MoO_3 are shown in Table 1.1.

Table 1.1 Physical properties of α–MoO_3.

Properties	Unit	MoO_3
Mineral name	–	Molybdite
Crystal structure	–	Orthorhombic
Space group	–	D_{2h}^{16}
Lattice constants	Å	a = 3.96 b = 13.86 c = 3.70
Density (ρ)	g cm^{-3}	4.69
Mohs hardness		3.5
Melting point	°C	795
Boiling point	°C	1155
Standard enthalpy of formation at 25°C (ΔH_f)	kJ·mol^{-1}	−745.17
Standard molar entropy at 298°C (S°)	J·(K·mol) $^{-1}$	77.78
Band gap	eV	3.0

Crytal structure

MoO_3 has two crystal structure phases, named monoclinic structure and orthorhombic structure. The monoclinic MoO_3 (β–MoO_3), thermodynamically metastable phase, can transform to the orthorhombic MoO_3 (α–MoO_3), which is a thermodynamically stable phase, at 400°C. The lattice parameters of the α–MoO_3 are **a**=3.96 Å, **b**=13.86 Å, and **c**=3.70 Å as shown in Fig. 1.3. This figure shows the crystal structure of the α–MoO_3 which composes of double layers of distorted MoO_6 octahedral held together by covalent forces in the **a** and **c** axis directions and by the weaker Van der Waals forces in the **b** axis direction. The chain and layer structures of MoO_3 are shown in Fig. 1.3a. Three inequivalent oxygen atoms, namely O1, O2, and O3, respectively, are shown in Fig. 1.3b. The Mo–O distances of the distorted octahedrons can be seen in Fig. 1.3c. The length of the shortest bond is 1.67 Å. This corresponds to the Mo–O1 bond. In the **a** axis direction, there are two Mo–O3 bonds with the distances of 2.23 Å and 1.73 Å, respectively. There are three bondings between O2 and Mo. Two equal bondings are along the **c** axis with the distance of 1.95 Å. The third bonding is in the **b** axis direction with the distance of 2.33 Å.

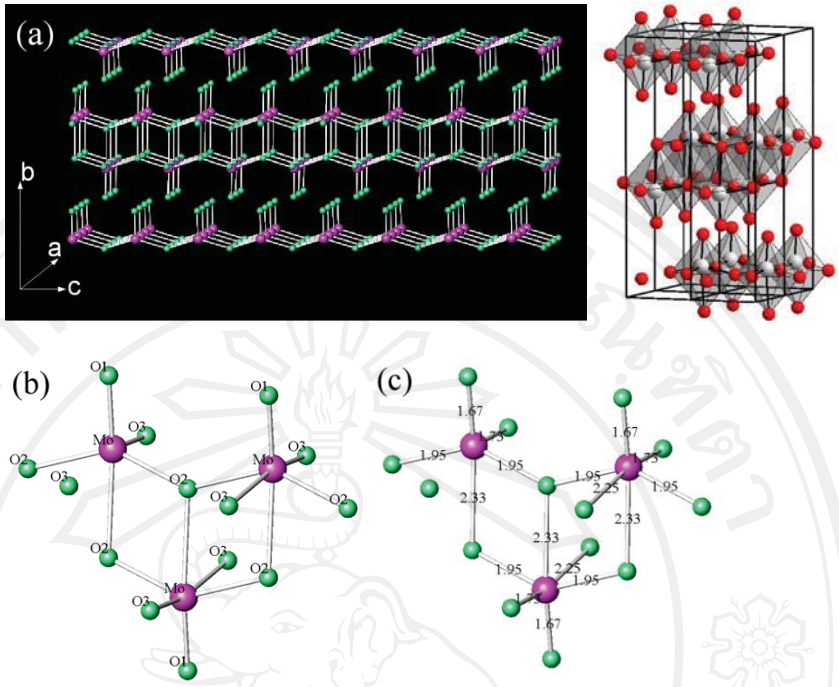

Figure 1.3 The α–MoO_3 crystal structure: (a) layer structure, (b) oxygen position, and (c) bond length [30, 31].

Lattice dynamic and Optical properties

There are sixteen atoms in a unit cell of the α–MoO_3 with the space group of D_{2h}^{16} [32]. Four atoms are molybdenum and the remainders are oxygen. This results in forty–eight eigenmodes at the center of Brillouin zone (q=0) which can be described by the displacements of the atoms. This could be either parallel or perpendicular to the chain axis **c**. The irreducible representation is given as

$$\Gamma = 8A_g+8B_{1g}+4B_{2g}+4B_{3g}+4A_u+3B_{1u}+7B_{2u}+7B_{3u} \qquad (1.1)$$

where A_g, B_{1g}, B_{2g}, and B_{3g} are Raman–active modes, A_u is an inactive mode, and the remainders are infrared–active modes.

Applications

MoO_3 is an interesting material for a variety of potential applications, such as catalysts, photoluminescence, photochromisms, electrochromisms, sensors, and batteries [33-38]. Because of its layered structure and the ease of the Mo(VI)/Mo(V) couple, MoO_3 is of interest in electrochemical devices and displays [39]. Much effort has been carried out to synthesize nanostructures of MoO_3 in order to improve its properties and to extend its applications.

1.2.2 Tin dioxide

Tin dioxide (SnO_2) is a metal oxide wide band gap semiconductor. The mineral form of SnO_2 is called "cassiterite," which is the most important raw material in tin chemistry. SnO_2 is water insoluble but can dissolve in acids. SnO_2 powder appears in white color and its single crystal is transparent. The melting and boiling point of SnO_2 are 1630°C and 1900°C, respectively. In industry, SnO_2 is used as a catalyst for the oxidation of aromatic compounds in the synthesis of carboxylic acids and anhydride acid. Physical properties of SnO_2 are shown in Table 1.2.

Table 1.2 Physical properties of SnO_2 [42].

Properties	Unit	SnO_2
Mineral name	–	Cassiterite
Abundance of the metal in the earth's crust	ppm	40
Crystal structure	–	Tetragonal, rutie
Space group	–	$P4_2mnm$
Lattice constants	Å	a = b = 4.74 c = 3.19
Density (ρ)	g cm^{-3}	6.99
Mohs hardness		6.5
Thermal expansion coefficient (300 K)	10^{-6} K^{-1}	|| c : 3.7 ⊥ c : 4.0
Melting point	°C	1900
Melting point of metal [°C]	°C	232
Vapor pressure of metal at 500 °C	Torr	5 x 10^{-9}
Standard enthalpy of formation at 25°C (ΔH_f)	kJ·mol^{-1}	−515.8
Standard molar entropy at 25°C (S°)	J·$(K·mol)^{-1}$	49.0
Band gap	eV	3.6
Static dielectric constant (ε_r)	–	|| c : 3.9 ⊥ c : 13.5
Effective electron mass of conduction electrons m^*/m_0 (experimental)	–	|| c : 0.23 ⊥ c : 0.3
Effective electron mass of conduction electrons m^*/m_0 (computational)	–	|| c : 0.20 ⊥ c : 0.26
Common extrinsic n−type dopants	–	Sb, F, Cl

Crystal structure

SnO_2 is also called "stannic oxide." It possesses the same rutile structure as many other metal oxides such as TiO_2, RuO_2, VO_2, and CrO_2. The crystal structure of SnO_2 is shown in Fig. 1.4. It has a tetragonal unit cell with lattice parameters of **a** = **b**

= 4.7374 Å, **c** = 3.1864 Å, **u** = 0.306. The parameter u, defined in Fig. 1.4, indicates the position of oxygen in the unit cell. This structure belongs to the point group symmetry 4/*mmn* and space group $P4_2/mnm$. There are two tin atoms and four oxygen atoms in a unit cell. The general position of atoms in the rutile structure can be defined as the basic vectors below:

$$B_1 = 0 \qquad \text{(Sn)}$$

$$B_2 = \frac{1}{2}\hat{a} + \frac{1}{2}\hat{b} + \frac{1}{2}\hat{c} \qquad \text{(Sn)}$$

$$B_3 = u\hat{a} + u\hat{b} \qquad \text{(O)}$$

$$B_4 = -u\hat{a} - u\hat{b} \qquad \text{(O)}$$

$$B_5 = (\frac{1}{2} + u)\hat{a} + (\frac{1}{2} - u)\hat{b} + \frac{1}{2}\hat{c} \qquad \text{(O)}$$

$$B_6 = (\frac{1}{2} - u)\hat{a} + (\frac{1}{2} + u)\hat{b} + \frac{1}{2}\hat{c} \qquad \text{(O)}$$

where $\hat{a}, \hat{b}, \hat{c}$ are unit vectors of **a**, **b**, **c** axis, respectively, u is a parameter as defined in Fig. 1.4

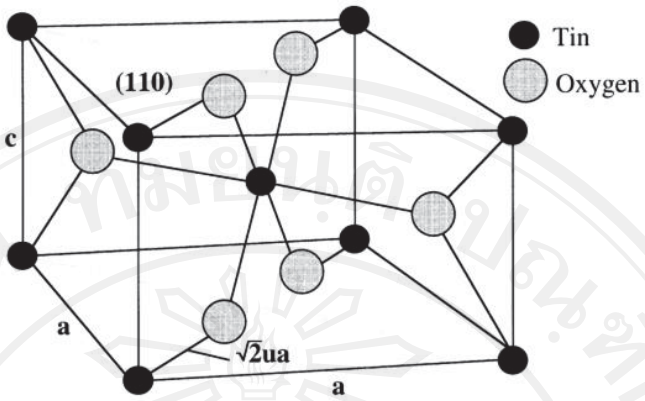

Figure 1.4 Primitive tetragonal unit cell of the SnO_2. The lattice parameter are **a** = 4.7374 Å, **c** = 3.1864 Å, and **u** = 0.306 [40].

Lattice dynamic and optical properties

There are six atoms in a unit cell, leading to 18 vibrational modes. The irreducible representation is given as

$$\Gamma = A_{1g} + A_{2g} + B_{1g} + B_{2g} + E_g + 2A_{2u} + 2B_{1u} + 4E_u \qquad (1.2)$$

Two modes are IR active (the single A_{2u} and the triple degenerated E_u mode), four modes are Raman active (three non−degenerate modes, A_{1g}, B_{1g}, and B_{2g} and the doubly degenerate E_g) and two are silent (A_{2g} and B_{1u}). One A_{2u} and two E_u modes are acoustic. The atomic displacements for Raman and IR−active modes are illustrated in Fig. 1.5.

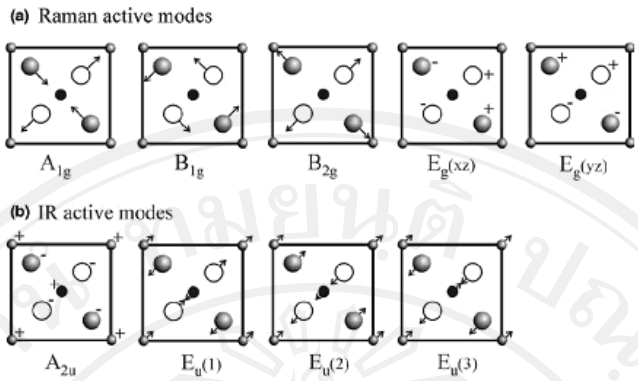

Figure 1.5 Schematic representation of atomic displacements for the Raman and IR–active modes of SnO_2 [41].

Applications

The applications of SnO_2 do not concern directly our daily life. Most important applications are in the advance technologies, such as electronic devices, smart windows, solar cell, and gas sensors. SnO_2 is the oxide material that combines low electronic resistance and high optical transparency for visible light. This leads to various advance devices. In the electronic device, SnO_2 is used as a material to fabricate light emitting diodes, transparent field effect transistors, and high voltage varistors. Due to the electrochromic property, SnO_2 is used to coat architectural windows to be smart windows which can control their coloring and transparency by applying a voltage across the film. SnO_2 is used as electrode materials for solar cells. In addition, commercial gas sensors based on SnO_2 are available due to the good sensitivity and stability. Due to lack of selectivity, many studies on gas sensing performance of nanoscaled SnO_2 have been carried out to improve the selectivity and also sensitivity.

1.3 Objectives and usefulness

1.2.1 Objectives

- To synthesize nanostructures of MoO_3 and SnO_2 by various techniques such as ion implantation and carbothermal reduction.

- To understand the electrical and optical properties of MoO_3 and SnO_2.

- To fabricate gas sensors with different characteristic by applying different material and morphology, or dopants and their gas sensing properties

- To fabricate array sensors by using different characteristic sensors

1.2.2 Usefulness

- The research will provide a technique to synthesize nanostructures of MoO_3 and SnO_2.

- The research will provide gas sensors based on SnO_2 nanostructures.

- The research will provide array sensor for e–nose application.